Inhibition of caspase-1-mediated inflammasome activation reduced blood coagulation in cerebrospinal fluid after subarachnoid haemorrhage

Yuanjian Fang,[a,#] Xiaoyu Wang,[a,#] Jianan Lu,[a,#] Hui Shi,[b] Lei Huang,[c,d] Anwen Shao,[a] Anke Zhang,[a] Yibo Liu,[a] Reng Ren,[a] Cameron Lenahan,[c,e] Jiping Tang,[c,d,f] Jianmin Zhang,[a]* John H. Zhang,[c,d,f]* and Sheng Chen [a]*

[a]Department of Neurosurgery, The Second Affiliated Hospital, School of Medicine, Zhejiang University, 88 Jiefang Road, Hangzhou, Zhejiang 310009, China
[b]Department of Neurosurgery, Yongchuan Hospital, Chongqing Medical University, Chongqing, China
[c]Department of Neurosurgery, Loma Linda University, 11041 Campus St, Risley Hall, Room 219, Loma Linda, CA 92354, United States
[d]Department of Physiology and Pharmacology, Loma Linda University, Loma Linda, CA, United States
[e]Burrell College of Osteopathic Medicine, Las Cruces, NM, United States
[f]Department of Anesthesiology, Loma Linda University, Loma Linda, CA, United States

Summary

Background Neuroinflammation and blood coagulation responses in cerebrospinal fluid (CSF) contribute to the poor outcome associated with subarachnoid haemorrhage (SAH). We explored the role of caspase-1-mediated inflammasome activation on extrinsic blood coagulation in CSF after SAH.

Methods Post-SAH proteomic changes and correlation between caspase-1 with extrinsic coagulation factors in human CSF after SAH were analysed. Time course and cell localisation of brain inflammasome and extrinsic coagulation proteins after SAH were explored in a rat SAH model. Pharmacological inhibition of caspase-1 via VX-765 was used to explore the role of caspase-1 in blood clearance and CSF circulation after SAH in rats. Primary astrocytes were used to evaluate the role of caspase-1 in haemoglobin-induced pyroptosis and tissue factor (TF) production/release.

Findings Neuroinflammation and blood coagulation activated after SAH in human CSF. The caspase-1 levels significantly correlated with the extrinsic coagulation factors. The activated caspase-1 and extrinsic coagulation initiator TF was increased on astrocytes after SAH in rats. VX-765 attenuated neurological deficits by accelerating CSF circulation and blood clearance through inhibiting pyroptotic neuroinflammation and TF-induced fibrin deposition in the short-term, and improved learning and memory capacity by preventing hippocampal neuronal loss and hydrocephalus in the long-term after SAH in rats. VX-765 reduced haemoglobin-induced pyroptosis and TF production/release in primary astrocytes.

Interpretation Inhibition of caspase-1 by VX-765 appears to be a potential treatment against neuroinflammation and blood coagulation in CSF after SAH.

Funding This study was supported by National Institutes of Health of United States of America, and National Natural Science Foundation of China.

Keywords: Subarachnoid haemorrhage; Caspase-1; Inflammasome; Blood coagulation; Pyroptosis

---

*Corresponding authors.
    E-mail addresses: zjm135@zju.edu.cn (J. Zhang), jhzhang@llu.edu (J.H. Zhang), saintchan@zju.edu.cn (S. Chen).
# Dr. Yuanjian Fang, Dr. Xiaoyu Wang and Dr. Jianan Lu contributed equally to this work.

Research in context

Evidence before this study

Neuroinflammation and blood coagulation responses in cerebrospinal fluid (CSF) contribute to the poor outcome after subarachnoid haemorrhage (SAH). Accumulating clinical and preclinical research has focused on anti-neuroinflammation and anti-blood coagulation in CSF after SAH in past decades. In addition, previous studies have suggested an extensive cross-talk between the blood coagulation system and the inflammatory system in the cardiovascular system.

Added value of this study

We demonstrated that caspase-1 serves as a promising therapeutic target connecting cerebral neuroinflammation and the blood coagulation response after SAH. The caspase-1 levels predicted levels of extrinsic coagulation factors in CSF and poor outcome after SAH in human. Pharmacological inhibition of caspase-1 via VX-765 attenuated neurological deficits by accelerating CSF circulation and blood clearance through inhibiting pyroptotic neuroinflammation and extrinsic coagulation initiator TF-induced fibrin deposition in the short-term, and improved learning and memory capacity by preventing hippocampal neuronal loss and hydrocephalus in the long-term after SAH in rats. Besides, we found that caspase-1-mediated TF production/release was facilitated in astrocytes after haemoglobin stimulation.

Implications of all the available evidence

Caspase-1 served as a promising therapeutic target connecting cerebral neuroinflammation and the blood coagulation response after SAH. Inhibition of caspase-1 by VX-765 appears to be a potential treatment against neuroinflammation and blood coagulation in CSF after SAH.

Introduction

Subarachnoid haemorrhage (SAH) is a severe subtype of stroke associated with high mortality and morbidity.[1] Evidence suggests that the thick and diffuse blood distribution in cerebrospinal fluid (CSF) is the main risk factor of severe clinical course and poor outcome in SAH patients.[2,3] Blood components with secondary products (such as coagulation and degradation products) trigger a series of pathophysiological changes in both the acute and chronic stages after SAH.[4] Surgical interventions, such as lumbar drainage (LD) and external ventricular drainage (EVD), are widely used in the current clinical setting to facilitate bloody CSF clearance in SAH patients. However, the benefit remains limited and there is a risk of infection.[5,6] A pharmacological strategy targeting the prevention of blood/coagulation product formation would accelerate CSF circulation and improve the clinical outcome of SAH patients.

The CSF circulation is severely disturbed in both acute and late phases after SAH, which directly leads to increased intracerebral pressure (ICP), decreased cerebral blood perfusion, brain oedema formation, and hydrocephalus.[7−10] The blood coagulation response to SAH in the subarachnoid space is considered the leading cause of CSF flow abnormalities,[2,3,8,9,11] which directly blocks the ventricular system and arachnoid granules with the resultant CSF retention and acute hydrocephalus.[12,13] The coagulation cascade leads to fibrin clotting and deposition in the subarachnoid space and perivascular space, which further blocks the CSF-interstitial fluid (ISF) exchange and induces cerebral vasospasm and the neuroinflammatory response.[8,9,11,14] Besides, fibrin deposition on the choroid plexus has also been suggested as the cause of CSF hypersecretion.[15] Fibrin can remain in CSF for up to 7 days, even in the absence of visible blood, which may account for the long-term impairment of CSF circulation.[11,16] Several clinical and pre-clinical studies have proven that the inhibition of coagulation initiator tissue factor (TF) or fibrin could reverse the SAH-induced CSF circulation hindrance and reduce the post-SAH incidence of complications.[8,11,17,18]

The neuroinflammatory response participates in both acute and chronic pathophysiology after SAH, which also contributes to the unfavourable short- and long-term outcomes of SAH patients.[19] Inflammasome complex consisting of NOD-like receptors and the caspase-1 enzyme plays an important role in the inflammatory response after SAH. The process of inflammasome activation and subsequent pyroptosis are initiated by the endogenous damage-associated molecular pattern (DAMP) stimulations after SAH.[20] The activation of caspase-1 represents the maturation of inflammasome, which triggers the maturation of interleukin (IL)−1β and IL-18, as well as the cleavage of Gasdermin D (GSDMD). The GSDMD cleavage promotes pore formation in the plasma membrane and further facilitates IL release and osmotic cell lysis, namely, pyroptosis.[21]

Increasing evidence suggests that there exists extensive cross-talk between the blood coagulation system and the inflammatory system in the cardiovascular system.[22] Blood coagulation could be initiated by the inflammatory response and coagulation in turn affects the inflammatory process.[23] TF expression is highly related to the inflammatory cytokine-mediated activations of Toll-like receptors and IL receptors.[24] A recent study identified caspase-1 inflammasome activation as a trigger for TF release from pyroptotic macrophages, which further induced blood clotting in vessels.[25] Although the brain expresses high levels of TF in astrocytes,[26] the mechanisms of brain TF release and its effects on the coagulation response in CSF remain unclear in the setting of SAH.

Herein, we propose caspase-1 as a link between neuroinflammation and blood coagulation in CSF after

SAH. Caspase-1 inflammasome activation would lead to neuroinflammation and astrocytic TF release via pyroptosis after SAH. The inhibition of caspase-1 could reduce the neuroinflammation and impaired CSF circulation induced after SAH.

Methods

Experiment design

The study included 6 sub-experiments (**Figure S1**). All animals were randomly assigned to different experimental groups by generating random numbers before surgery. Sample size for each sub-experiment was designed according to our previous study.[27] Additional animals were supplied to meet the pre-determined sample size (n) after subjects were excluded. The inclusion and exclusion criteria are described in the following section. Information of experimental groups was blinded to researchers who collected and evaluated patients' information, and who performed animal surgeries, outcome assessments, and data analysis. Information of main reagents used in this study was listed in the **Table S1**.

Experiment 1. Relationship between inflammasome and blood coagulation response in human CSF after SAH.

Mass spectrometry analysis was used for comparison of proteomic differences within CSF between Control and SAH patients (n = 4/group). Thirty-six additional SAH patients were used to explore the relationship between inflammasomes and the blood coagulation response in CSF after SAH. Enzyme-linked immunosorbent assay (ELISA) was performed to measure the levels of caspase-1, TF, Fibrin, Thrombin-Antithrombin (TAT), and IL-1β. The high and low caspase-1 groups were divided according to the median caspase-1 level. Baseline data, clinical data, treatment, levels of TF, Fibrin, TAT, and IL-1β, and outcome at discharge were compared.

Experiment 2. Time course and cell localisation of inflammasome- and blood coagulation-related proteins in the ipsilateral hemisphere after SAH in rats.

Rats were assigned to the following 8 groups (n = 6/group): Sham, SAH-3 h, SAH-6 h, SAH-12 h, SAH-24 h, SAH-72 h, SAH-7 d, and SAH-14 d Western blots were used to evaluate the protein changes of caspase-1, TF, fibrin, IL-1β, and IL-18 in ipsilateral hemisphere brain tissues after SAH. Additionally, rats from Sham, SAH-24 h, SAH-72 h, and SAH-7 d (n = 4/group) were used for double immunofluorescence staining to explore cell localisation and quantification of caspase-1 p20 and TF.

Experiment 3. Effect of caspase-1 inhibition on short-term neurological outcome after SAH in rats.

This section was divided into two sub-experiments. 1) To determine the best dosage of VX-765. Rats were randomly assigned to Sham, SAH+DMSO, SAH+VX-765 (0.2 mg/kg), SAH+VX-765 (0.6 mg/kg), and SAH+VX-765 (1.8 mg/kg), and further assigned to 24 h and 72 h groups (n = 6/group). Neurological tests and brain water content were assessed to select the best dosage of VX-765 for the following study. 2) To explore the role of caspase-1 in CSF circulation after SAH. Rats were assigned to Sham, SAH+DMSO, and SAH+VX-765 to visualise CSF circulation in 24 h and 72 h after SAH (n = 4/group). Evans blue (EB) cisterna magna injection was used to visualise the CSF circulation. The SAH score was recorded for each rat to compare the blood clearance. Additionally, rats from Sham, SAH+DMSO, and SAH+VX-765 groups (n = 6/group) underwent the cisterna magna autologous blood injection model to compare blood clearance through haemoglobin assay in 24 h and 72 h after SAH.

Experiment 4. Effect of caspase-1 inhibition in neuroinflammation and blood coagulation response in the brain after SAH in rats.

Rats were assigned to Sham, SAH+DMSO, and SAH+VX-765. Immunofluorescence staining (n = 5/group) and western blot/ELISA (n = 6/group) were used to measure neuroinflammation and the blood coagulation response-related proteins at 72 h after SAH. In addition, extra rats were randomly assigned to Sham+Control CRISPR, Sham+GSDMD KO. CRISPR, SAH+Control CRISPR, and SAH+GSDMD KO. CRISPR (n = 6/group). Western blot was used to explore the GSDMD-mediated pro-neuroinflammation and pro-coagulation effects at 72 h after SAH.

Experiment 5. Effect of caspase-1 inhibition on long-term neurological outcome after SAH in rats.

Rats were randomly assigned to Sham, SAH+DMSO, and SAH+VX-765 (n = 10/group). The rotarod tests were conducted on days 7, 14, and 21 after SAH. The Morris water maze was conducted on days 23 to 28 after SAH. Nissl staining was conducted to assess the ipsilateral hippocampal neuron loss, cerebral ventricular volumes, and cortical thickness for post-SAH hydrocephalus on day 28 after SAH.

Experiment 6. Effect of caspase-1 inhibition on haemoglobin-treated primary astrocyte cultures.

This part was divided into two sub-experiments. 1) To explore the role of caspase-1-mediated inflammasome activation and TF release in primary astrocytes after haemoglobin. Three groups were divided: Sham, Haemoglobin +DMSO, and Haemoglobin+VX-765. CCK-8 assay was used to measure cell viability. Lactate dehydrogenase (LDH) release assay and flow cytometry of activated caspase-1 and PI were used to measure pyroptosis. Western

blot was used to determine the production and release of cytokines and TF after haemoglobin induction. 2) To explore the GSDMD- and IL-1β receptor 1 (IL-1R1)-mediated pro-neuroinflammatory and pro-coagulation effects. The control group and haemoglobin group were each treated with control CRISPR, GSDMD KO. CRISPR, and IL-1R1 KO. CRISPR. Western blot was used to determine the production and release of cytokines and TF after haemoglobin induction.

Clinical sample collection and patient information

Patients with aneurysmal SAH were diagnosed by computed tomography (CT) and digital subtraction angiography performed within 24 h after admissions. The inclusion criterion was defined as SAH patients with modified Fisher Scale 3−4. Patients with a history of central nervous system (CNS) diseases (e.g., stroke, traumatic brain injury, CNS infection) or accompanied by serious comorbidities before SAH onset (e.g., severe coagulation disorders, malignant tumour, uncontrollable heart disease, and hypertension) or other organ dysfunctions within 6 months were excluded from the study. All CSF samples of SAH patients were collected before coiling or clipping through lumbar puncture or LD or EVD within 48 h after SAH. All CSF samples of the control group were obtained from intraspinal anaesthesia before surgery in patients with non-neurological diseases. The CSF samples were centrifuged at 3000 r/min for 10 min at 4 °C to remove cells in CSF, and stored at −80 °C until assayed.

All patients were treated according to the guidelines proposed by the Neurocritical Care Society and American Heart Association as our previous study.[28] Baseline data of patients, including age, sex, body mass index (BMI), history of hypertension and diabetes were collected; Clinical data, including Hunt-Hess score, Subarachnoid hemorrhage Early Brain edema Score (SEBES), and blood clot formation (CT attenuation higher above 70UI[29] on CT or finding in surgery) were evaluated on admission; Treatment including LD, EVD, coiling, and clipping were collected; Laboratory data of coagulation and inflammasome responses were examined by ELISA; SAH-related complications included delayed cerebral ischaemia [defined as clinical cerebral vasospasm (clinical deterioration that excluded other causes)], cerebral infarction (new cerebral infarction appeared on CT or MRI, which should exclude infarctions that appear within 48 h after surgery or coiling), and hydrocephalus. Functional outcomes at discharge were evaluated by length of hospital stay and neurological score modified Rankin Scale (mRS).

Mass spectrometry of human CSF

Mass spectrometry was carried out at LC Sciences (Hangzhou, Zhejiang, China). The most abundant proteins (from serum and plasma) in the CSF sample were depleted using Agilent Human 14 Multiple Affinity Removal System Column (Agilent Technologies, Santa Clara, CA, USA). The remaining samples were then quantified with the BCA assay (Bio-Rad, Hercules, CA, USA). The protein preparation procedure used the filter-aided sample preparation (FASP) method (44). Peptide mixture was labelled using TMT reagent according to the manufacturer's instructions (Thermo Fisher Scientific, Waltham, MA, USA). TMT-labelled peptides were fractionated by RP chromatography using the Agilent 1260 infinity II HPLC system (Thermo Fisher Scientific). Each fraction was injected for nanoLC-MS/MS analysis, followed by LC-MS/MS analysis performed on a Q Exactive plus mass spectrometer (Thermo Fisher Scientific). MASCOT engine (Matrix Science, London, UK; version 2.6) embedded into Proteome Discoverer 2.2 (Thermo Fisher Scientific), was used for raw data acquisition and quantification.

ELISA assay

The concentrations of CSF coagulation factors and cytokines were determined using ELISA kits. Human CSF samples (100 μl) were used for the analysis. Rat CSF samples (100 μl) were derived from cisterna magna for the analysis. All procedures were performed according to the manufacturer's instruction.

Animals

Adult male Sprague-Dawley rats weighing 280−320 g were used for this experiment. All rats were housed in a humidity- and temperature-controlled facility, with a 12-hour light/dark cycle, and ad libitum access to water and standard rodent chow.

Astrocyte cultures

Primary astrocyte cultures were prepared from newborn Sprague Dawley rats (SLAC, Shanghai, China, RRID: MGI:5651135), as previously described.[30] Briefly, the rats were decapitated for sterilisation. Brain cortices were dissected and removed with meninges blood vessels and hippocampus. The brain cortices were trypsinised and dissociated via gentle trituration. Suspensions were collected and centrifuged. The cell pellets were re-suspended in culture medium (Dulbecco's modified Eagle's medium (Thermo Fisher Scientific) with 10% foetal bovine serum, penicillin G, and streptomycin) and seeded into poly-D-lysine-coated 75cm² flasks. Cells were cultured at 37 °C in 95% humidity with 5% CO₂. Microglia and oligodendrocyte progenitors were removed by shaking the flask at 220 rpm for 1 h at 37 °C. The secondary astrocytes were used in the experiments. Immunofluorescence staining of astrocytes and microglia were conducted to ensure the purity of astrocytes.

SAH model

Animal models. The endovascular perforation model was the primary model of SAH induction in this study, which was performed according to our previous study.[27] Briefly, the rats were intubated under isoflurane anaesthesia and mechanically ventilated. Haemorrhage was induced by a sharp 4−0 monofilament, which was inserted from the left external carotid artery to the internal carotid artery. The monofilament then punctured the bifurcation of the anterior and middle cerebral arteries. Sham animals underwent the same procedures, but without vessel puncture.

The cisterna magna autologous blood injection model of SAH was performed as previously described,[31] but was only used in Experiment 3. The rats were anesthetised with isoflurane, and we collected 300 μl of arterial blood from the left ventricle. Next, blood was injected over 15 s through a catheter placed in the cisterna magna. The Sham animals received saline solution.

Vital signs, including respiratory rate, heart rate, skin pigmentation, and pedal reflex, were recorded intraoperatively every 5 min to confirm the anaesthetic status and to prevent distress and excessive pain during surgery. Buprenorphine was used depending on the degree of observed distress or pain, and given for 6 hours-1 day depending on signs of pain or distress. The first administration of buprenorphine (0.02 mg/kg) was injected subcutaneously before anaesthesia and rats were observed for any sign of pain or distress. Animals dead before outcome assessments were excluded.

In vitro model. Primary astrocytes were cultured with 25 μM haemoglobin (MilliporeSigma, Burlington, MA, USA) resolved with culture medium for 24 h to mimic SAH conditions.[30]

SAH severity

SAH Grade. The SAH grade was blindly evaluated by two independent investigators according to the previous study.[32] The basal cistern was divided into six segments, and were scored from 0 to 3 according to the thickness of the blood clot. The final score combined all segments and ranged from 0 to 18. A higher score represents an increased blood volume.

Haemoglobin assay. A modified spectrophotometric haemoglobin assay was used according to the previous study.[33] Briefly, the brain was homogenised with 3 mL PBS and centrifuged at 13,000 rpm for 30 min. The supernatant was immediately transferred to a clean tube with a 4:1 ratio of Drabkin's reagent (Sigma-Aldrich, St. Louis, MO, USA) and incubated for 15 min. absorbence of sample was analysed on a standard curve by spectrophotometric measurements at 540 nm wavelength (Thermo Spectronic Genesys 10 UV, Thermo Fischer Scientific).

Drug administration

For the in vivo experiment, two routes of administration, including intracerebroventricular (i.c.v.) and intranasal (i.n.) routes, were utilised. The detailed procedure was conducted as previously described.[27,34] The caspase-1 selective inhibitor, VX-765 (compound structure see[35]), was dissolved in dimethyl sulfoxide (DMSO) and corn oil, and was given (i.n.) at 1 h, 25 h, and 49 h after surgery. All CRISPRs used in vivo were administered (2 μg/rat, i.c.v.) with a transfection reagent at 48 h before SAH.

For the in vitro experiments, the primary astrocytes were pre-treated with VX-765 at concentrations of 25 μM, 50 μM, and 100 μM 1 h before haemoglobin stimulation according to the previous study.[36] All CRISPRs were given 2 μg/well and transfected with a transfection reagent at 48 h before haemoglobin stimulation.

The engineered form of CRISPR-associated (Cas9) protein system designed by Santa Cruz Biotechnology (Dallas, TX, USA) was used to inactivate target genes.[27] The CRISPR protein Cas9 is directed to genomic target sites by short guide RNAs, where it functions as an endonuclease and further inactivates or activates the targeted gene. GSDMD knockout CRISPR: TGAAGCTGGTAGAATTCCGA; TGCGTGTGACTCAGCAGACC; TCGTGGGGATGACGTGTTTG. IL-1R1 knockout CRISPR: AGTCCCGGTCCGCTGATATG; GCCGTATGTCCTATACGTTC; TTGCTTCCCCCGG AACGTAT. Control CRISPR was administered to avoid potential bias carried by the off-target effects of the CRISPR system. The effect of CRISPR system was determined by western blot.

Cell viability assay and cytotoxicity assay

Cell viability was measured using the CCK-8 cell counting kit according to the manufacturer's instruction. Cell cytotoxicity, as determined by LDH concentration in cell culture supernatant, was measured using the LDH cytotoxicity test kit according to the manufacturer's instructions. Each individual treatment reflects four replicates for all assays in plates.

Neurobehavior assessment

Short-term Assessment. The Modified Garcia (ranging from 0 to 18) and Beam Balance tests (ranging from 0 to 4) were conducted to evaluate the short-term neurological function, including response capacity, alertness,

coordination, motor skills, complex movements, and coordination.[27] A higher score represents better neurological function.

Long-term Assessment. The rotarod test was conducted on days 7, 14, and 21 post-SAH to evaluate the sensorimotor coordination and balance capacity as previously described.[27] The initial rotating speed was set at either 5 or 10 rpm (RPM) and accelerated by 2 RPM every 5 s. Each animal was allowed to run 5 times on test day (with a one-minute interval between each run). The results were recorded as the average duration on the rotarod.

The Morris water maze tests were conducted on days 23 to 28 after SAH to assess the capacity of spatial learning and memory as previously described.[27] The swim path, escape latency, and swim distance to reach the submerged platform were recorded individually on days 23 to 27 post-SAH. The platform was removed at 28 days post-SAH. The 60-s probe test was conducted to record the swimming speed and duration of time spent in the probe quadrant. All tests were recorded by the Computer Tracking System (San Diego Instruments Inc., San Diego, CA).

Intracerebral pressure measurement
Under deep anaesthesia, the rats were placed in a stereotactic frame in a head-down position, and a parietooccipital incision was made. After exposure of the parietooccipital membrane, a PE-50 catheter (Becton Dickinson, Franklin Lakes, NJ) filled with artificial CSF was gently inserted into the cisterna magna (2 to 3 mm depth) and fixed with dental cement and cyanoacrylate glue to prevent potential CSF leakage. The data was recorded after ICP equilibration using the WINDAQ data-acquisition system (DATAQ, Akron, OH).

Brain water content
Wet-dry weight measurement for brain oedema was performed as previously described.[27] Briefly, brain water content (%) was calculated as follows: [(wet weight-dry weight)/wet weight*100%].

CSF movement tracking
Evans blue (EB) dye cisterna magna injection was performed to visualise the CSF movement and clearance as previously described.[27,37] Briefly, a precision 50-μl Hamilton syringe needle (Hamilton Company Inc., Reno, NV) was inserted into the cisterna magna. The needle was also fixed with dental cement and cyanoacrylate glue to prevent potential CSF leakage. Next, 25 μl of 2% EB dye (Sigma-Aldrich) was injected within 25 min at a rate of 1 μl/min, and was allowed to circulate for another 35 min. The rats were sacrificed after transcardiac perfusion of PBS (0.01 M) at 60 min after the start of EB injection. Quantification of CSF movement speed was determined by the distribution of EB on the ventral surface of the brain, and the concentration of EB in the forebrain.

The concentration of EB in blood and deep cervical lymph nodes (dcLNs) were analysed to show the CSF clearance speed from the subarachnoid space to blood and peripheral lymph nodes. Blood samples were collected from the femoral vein at 60 min after the start of EB injection. Deep cervical lymph nodes (dcLNs) were collected at 60 min after the start of EB injection.

For measuring EB concentration, all samples were homogenised or mixed with 50% trichloroacetic acid (Sigma-Aldrich), and were then incubated at 4 °C overnight. On the second day, the samples were centrifuged at 15,000 RPM at 4 °C for 30 min. The supernatant was analysed on a standard curve by spectrophotometric measurements at 610 nm wavelength (Thermo Spectronic Genesys 10 UV, Thermo Fischer Scientific).

Histological staining
Brain processing of histological staining was conducted as previously described.[27] Briefly, the rats were deeply anesthetised and transcardially perfused with PBS (0.01 M) and 10% neutral buffered formalin before decapitation. The brains were fixed with 10% formalin for 24 h, 4% paraformaldehyde for another 24 h, and then cryoprotected with serial 15 and 30% sucrose solutions for 2−4 days. For histological staining of the brain slices, 10- to 15-μm-thick coronal frozen slices were prepared.

Whole brain immunofluorescence. The whole brain immunofluorescence of fibrin was conducted for visualisation of the Fibrin deposition on the brain surface. Brains were incubated with 0.3% Triton X-100 for 30 min and blocked with 5% normal donkey serum for 3 h at room temperature. After blocking, brains were incubated overnight with anti-fibrinogen antibody. On the second day, the brains were incubated with secondary antibodies conjugated with Alexa Fluor 488 and visualised using a chemiluminescence detection system (IVIS spectrum, Perkin Elmer, Waltham, MA, USA).

Double Immunofluorescence. The brain slices (10 μm) were used for double immunofluorescence. Briefly, the brain slices were incubated with 0.3% Triton X-100 for 30 min and 5% normal donkey serum for 1 h at room temperature, followed by incubation with primary antibodies overnight at 4 °C. On the second day, the brain slices were incubated with species-corresponding fluorescence-conjugated secondary antibodies or TUNEL staining kit for 1 h at room temperature. The images were visualised and photographed using a fluorescence

microscope (Leica Microsystems, Wetzlar, Germany). The quantification of positive cells was averaged from nine randomised areas from three different brain sections (three randomised areas of each section).

Immunohistochemical Staining of Fibrin. The brain slices (12 μm) were used for immunohistochemical staining of fibrin according to our previous study.[27] Briefly, the brain slices were incubated with 0.3% Triton X-100 for 30 min, 1% hydrogen peroxide (H_2O_2) for 15 min, and 5% normal donkey serum for 1 h at room temperature, followed by incubation with rabbit anti-fibrinogen antibody overnight at 4 °C. On the second day, the brain slices were incubated with biotinylated anti-rabbit antibody for 1 h at room temperature, followed by 30 min incubation of ABC Reagent. colour reactions were performed with peroxidase substrate solution and hematoxylin. Images of the cortex, middle cerebral artery (MCA), perivascular space in hypothalamus, and choroid plexus were photographed using an optical microscope (Olympus, center Valley, PA). Quantification of fibrin deposition was measured using ImageJ software (ImageJ, version 15.1, NIH, Bethesda, MD, USA), and averaged from four different sections.

Nissl Staining. Brain slices (15 μm) were used for Nissl staining as previously described.[27] Briefly, the brain slices were submerged in 0.5% cresyl violet solution at the desired stain intensity, and was then dehydrated with 100% alcohol.

Hydrocephalus was measured by the cortical thickness and ventricular volume. Cortical thickness and the ventricular area were analysed at the level of the pre-optic chiasm, fornix-hippocampus commissure, and rear hippocampus using the ImageJ software. Ventricular volumes were calculated using the following formula: average ventricular area at various levels * total section thickness.

Microphotographs of ipsilateral (left) hippocampal regions were captured to visualise surviving neuron in the hippocampus. Quantification of neuronal loss was analysed using ImageJ software in the cornu ammonis (CA)1 area (at 20X magnification) and was averaged from three brain sections.

Determination of pyroptosis

For the in vivo experiment, cells that underwent pyroptosis were identified by TUNEL staining and immuno-fluorescence staining of caspase-1 p20. The detailed procedure was conducted according to the "Double Immunofluorescence" section. Caspase-1 p20- and TUNEL-positive cells were determined to be pyroptotic cells.

For the in vitro experiment, FAM-FLICA Caspase-1 Assay Kit was used to detect activated caspase-1 and PI

in primary astrocyte cultures as previously described.[38] All procedures were performed according to the manufacturer's instructions. Stained cells were analysed via flow cytometry (FACSCalibur; BD Biosciences, San Diego, CA, USA).

Western blot

The protein samples were extracted from brain tissues (ipsilateral cerebral hemisphere), primary cultured astrocytes, or cell-free culture supernatant (serum-free media) for immunoblotting analysis. All samples were added to the proteinase inhibitor and halt phosphatase inhibitor cocktail (Thermo Scientific). Protein concentrations were measured using a BCA protein kit (Thermo Scientific).

The samples (20 μg protein per lane) were loaded onto 7.5−12% SDS-PAGE gels. After electrophoresis, the proteins were transferred to nitrocellulose membranes (0.22 μm). The membrane was incubated with blocking buffer (5% no-fat milk) for 1 h at room temperature, followed with overnight incubation with the primary antibody at 4 °C. On the second day, the species-corresponding secondary antibodies were incubated with the membrane at room temperature for 1 h. Next, the immunoblots were visualised using the ECL Plus chemiluminescence re-agent kit (Amersham Bioscience, Pittsburgh, PA). Quantification was conducted by the ImageJ software.

Statistics

Data are presented as mean ± standard deviation (SD) or number (percentage). Statistical analysis was conducted using GraphPad Prism 8.2.1 (GraphPad Software, San Diego, CA, USA) and SPSS 23.0 (IBM, Armonk, NY, USA). Adjusted P-value was used for multiple testing. $P < 0.05$ was considered statistically significant.

In experiment 1, the caspase-1 categories were divided by the median value of the caspase-1 levels in CSF. Continuous variables were tested using unpaired Student's t tests, and categorical variables were tested using chi-square or Fisher's exact tests.

In statistical analysis of mass spectrometry, proteins with Fold change > 1.2 and P value (Student's t-test) < 0.05 were considered differentially expressed proteins. Gene set enrichment analysis (GSEA) was performed according to the Gene Ontology (GO) classification on http://geneontology.org. The enrichment score curve is the running sum of the weighted enrichment score generated by the GSEA software. A gene set with false discovery rate (FDR) < 0.25, |normalised enrichment scores (NES)| > 1, and nominal (NOM) p value < 0.05 was recognised as statistically significant.

In experiments 2−6, Shapiro-Wilk test was used to test the normality, and variables were log transformed
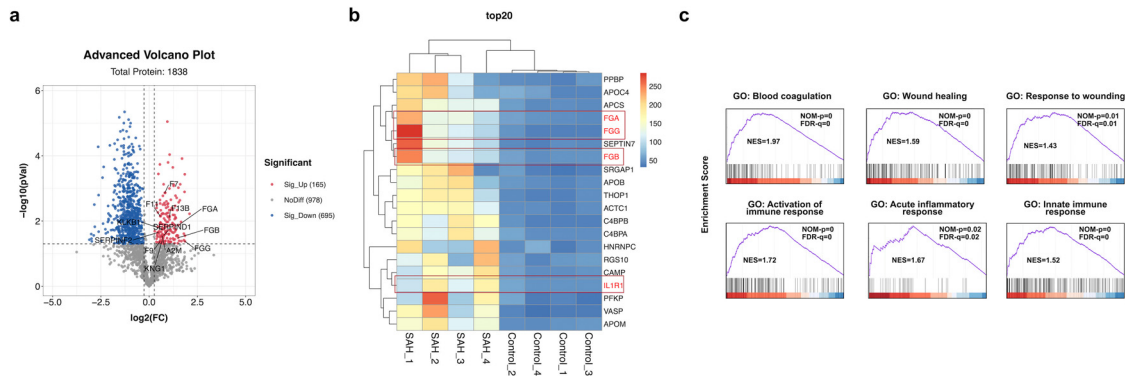
Figure 1. The blood coagulation and neuroinflammatory response in human CSF after SAH. a. Differentially expressed proteins in human CSF after SAH measured by mass spectrometry. There were 860 proteins differentially expressed. Of which, 165 were upregulated and 695 were downregulated. The upregulated coagulation-related proteins are listed as follows: coagulation factor VII (F7), coagulation factor IX (F9), coagulation factor XI (F11), coagulation factor XIII (F13B), fibrinogen alpha chain (FGA), fibrinogen beta chain (FGB), fibrinogen gamma chain (FGG), Kallikrein B1 (KLKB1), Serpin Family D Member 1 (SERPIND1), Serpin Family F Member 2 (SERPINF2), alpha-2-Macroglobulin (A2M), and Kininogen 1 (KNG1). **b.** Heat map list of the top 20 upregulated proteins in human CSF response to SAH. The FGA, FGB, FGG, and IL-1R1 (red box) were significantly upregulated. **c.** GSEA results of neuroinflammation- and coagulation-related GO pathways.

when necessary. Based on the distribution of normality, one-way ANOVA, followed by Tukey's post hoc test, was used to compare multiple groups. Two-way ANOVA, followed by Tukey's post hoc test was used to compare the changes according to the different levels of multiple categorical variables (e.g. comparison of brain water content or long-term outcomes in different groups). The Kruskal-Wallis test was used to compare the difference of data in non-Gaussian distribution. Log-rank (Mantel-Cox) test was used to compare the difference between survival curves.

Ethics
All studies concerning human information and tissues were approved by the Ethics Committee of the Second Affiliated Hospital of Zhejiang University School of Medicine (No.2020−892), and is registered as an observational study in *ClinicalTrail.gov* (No.NCT04938414).[39] All of the patients signed informed consent.

All experimental procedures involving animals were approved by the Institutional Animal Care and Use Committee of Loma Linda University (protocol No. 20−010), and were conducted in compliance with protocols established by the National Institutes of Health Guide for the Care and Use of Laboratory Animals.

Role of funding source
The funders had no role in the study design, collection, analysis and interpretation of data, manuscript preparation, and the decision to submit the paper for publication.

Results
Forty patients with severe SAH (mFS 3−4) and four control patients were included in the human experiment. The age of SAH patients was 58.0 ± 12.6 (ranging from 18 to 85), with 18 male and 22 female. The age of SAH control patients was 55.0 ± 7.4 (ranging from 45 to 62), with 2 male and 2 female.

A total of 312 male SD rats were used in the animal experiments, with 75 and 237 undergoing Sham surgery and SAH surgery, respectively. The total mortality of the SAH rats was 17.3% (41/237) with mortality details of each group listed in the **Table S2**.

Inflammasome and blood coagulation activation correlated with caspase-1 levels in human CSF after SAH
To identify the dysregulated proteins in human CSF after SAH, 1838 unique proteins were identified amongst CSF samples. Of which, 860 were differentially expressed (165 upregulated and 695 downregulated) in CSF from SAH patients compared to normal control. Both intrinsic and extrinsic coagulation cascade factors (e.g. coagulation factors VII, IX, XI, and fibrinogen chains) were significantly upregulated after SAH (Figure 1a). Clustering analysis showed the fibrinogen alpha chain, fibrinogen beta chain, fibrinogen gamma chain, and IL-1R1 were amongst the top 20 upregulated proteins in CSF after SAH (Figure 1b). In addition, GSEA showed that the proteins related to blood coagulation, wounding, and the immune inflammatory response were enriched in the CSF after SAH (Figure 1c), which highlighted the role of inflammatory and

	Low caspase-1* (n = 18)	High caspase-1* (n = 18)	P-value
Baseline data			
Age	57.2 ± 9.4	58.8 ± 15.1	0.704
Female	12 (66.7)	10 (55.6)	0.733
Body mass index	23.0 ± 3.5	24.3 ± 3.1	0.204
Hypertension	8 (44.4)	11 (61.1)	0.505
Diabetes	1 (5.6)	1 (5.6)	>0.999
Clinical data			
High Hunt-Hess (3—4)	4 (22.2)	13 (72.2)	0.007
High SEBES (3—4)	9 (50.0)	17 (94.4)	0.007
Blood Clot	8 (44.4)	16 (88.9)	0.012
Treatment			
LD	14 (77.8)	13 (72.2)	>0.999
EVD	3 (16.7)	7 (38.9)	0.264
Clipping	13 (72.2)	10 (55.6)	0.489
Coiling	5 (27.8)	8 (44.4)	0.489
Laboratory data (CSF)			
TF (pg/ml)	221.1 ± 184.0	372.7 ± 157.2	**0.012**
TAT (pg/ml)	52.5 ± 48.1	93.3 ± 35.8	**0.007**
Fibrinogen (ng/ml)	935.3 ± 180.9	1093.5 ± 155.2	**0.008**
IL-1β (pg/ml)	11.25±7.3	44.98±27.3	**<0.001**
Complications			
Delayed cerebral ischaemia	7 (38.9)	15 (83.3)	**0.015**
Hydrocephalus	2 (11.1)	9 (50.0)	**0.027**
Outcome at discharge			
Length of hospital stay	16.0 ± 9.3	20.4 ± 16.2	0.325
Unfavourable mRS (3—5)	7 (38.9)	14 (77.8)	**0.041**

Table 1: The correlation between CSF caspase-1 levels with clinical severity, CSF coagulation, inflammatory response, and outcome in patients with severe SAH (mFS 3—4).
  * Categories of caspase-1 groups will be divided by the median value (106.1pg/ml).Data presented as n (%) or mean±SD. Continuous variables were tested using unpaired Student's t tests, and categorical variables were tested using chi-square or Fisher's exact tests.

coagulation response after SAH. However, caspase-1, inflammatory cytokines, and TF were not detected in the CSF by mass spectrometry, which may be due to the low sensitivity of mass spectrum.

The levels of caspase-1, TF, TAT, Fibrin, and IL-1β in CSF samples from 36 SAH patients were further evaluated by ELISA (Table 1). The patients were divided into Low caspase-1 and High caspase-1 groups according to the median caspase-1 levels (106.1pg/ml). No statistical significance was found between the two groups regarding baseline data and treatment (both $P > 0.203$, Fisher's exact test and unpaired Student's t-test). Patients in the High caspase-1 group presented with higher Hunt-Hess score and SEBES,[40] as well as a higher incidence of clots formation compared to the Low caspase-1 group ($P<0.013$, Fisher's exact test). The levels of TF, TAT, Fibrin, and IL-1β in CSF were also higher in the High caspase group compared to the Low caspase-1 group ($P < 0.013$, unpaired Student's t-test). Additionally, despite no statistical significance being found in length of hospital stay ($P = 0.325$, unpaired Student's t-test), those patients with higher caspase-1 levels in CSF had higher incidence of DCI and hydrocephalus, as well as worse outcome scores at discharge compared to the Low caspase-1 group ($P<0.042$, Fisher's exact test).

Time course and cell location of inflammasome- and coagulation-related proteins after SAH in rats

To explore the time course and cell location of inflammasome- and coagulation-related proteins in the ipsilateral hemisphere after SAH, the rat model of endovascular perforation was conducted. As shown (Figure 2a,b), the protein levels of caspase-1 p50 were significantly increased from 12 h to 72 h, and peaked at 72 h after SAH when compared to the Sham group ($P<0.046$, one-way ANOVA, Tukey's post hoc test). The cleaved form of caspase-p20 was significantly increased from 24 h to 14 d, and peaked at 72 h after SAH when compared to the Sham group ($P < 0.017$, one-way ANOVA, Tukey's post hoc test). Similarly, the inflammasome-related cytokines, IL-1β and IL-18, were markedly increased from 24 h to 7 d after SAH when compared with Sham group ($P<0.031$, one-way ANOVA, Tukey's post hoc test). The extrinsic coagulation initiator TF was markedly increased from 12 h to 7
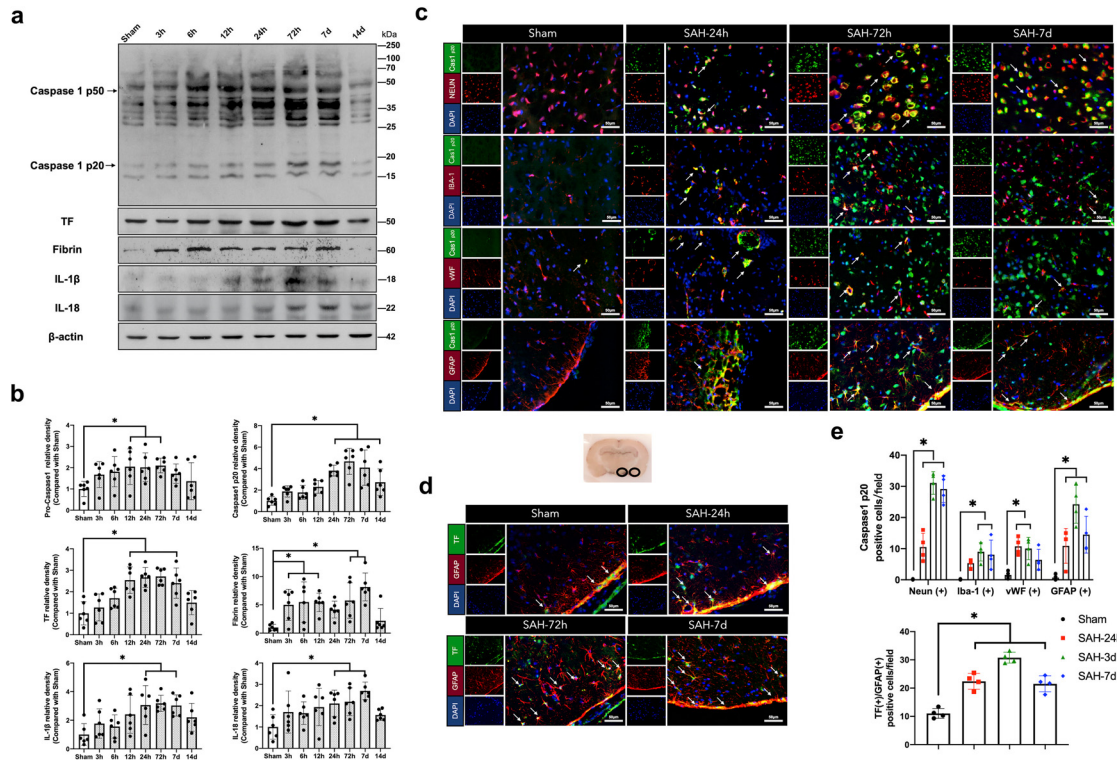
Figure 2. Time course and cell location of inflammasome- and blood coagulation-related proteins after SAH in rats. a-b. Representative western blot bands and densitometric quantification of caspase-1, TF, Fibrin, IL-1β, and IL-18 in ipsilateral hemisphere. The relative level of each protein was normalised to β-actin from the same sample. n = 6 per group **c-d.** Representative microphotographs of co-immunofluorescence staining of caspase-1 p20 (green) with neurons (NeuN, red), astrocytes (GFAP, red), and endothelial cells (vWF, red); TF (green) with astrocytes (GFAP, red) in the ipsilateral basal cortex of Sham, SAH (24 h), SAH (72 h), and SAH (7d). Scale bar=50 μm. **e.** Quantification of caspase-1 p20- or TF-positive cells. Positive cells were counted and averaged from three randomised areas chosen in the microphotographs of ipsilateral cortex. n = 4 per group. All data are presented as mean ± SD. *$P<0.05$, One-way ANOVA, Tukey's post hoc test.

d, and peaked at 72 h after SAH when compared to Sham ($P<0.001$, one-way ANOVA, Tukey's post hoc test). Meanwhile, the clotting components, fibrin, was significantly increased from 3 h to 12 h and from 72 h to 7 d after SAH when compared to Sham group ($P<0.035$, one-way ANOVA, Tukey's post hoc test).

The double immunofluorescence staining was conducted at 24 h, 72 h, and 7 d after SAH to detect the spatial distribution changes of caspase-1 p20 and TF in the ipsilateral hemisphere after SAH. As shown in Figure 2c, the caspase-1 p20-positive neurons, microglia, endothelial cells, and astrocytes were mainly observed near the site of artery rupture (puncture site) at 24 h after SAH. There was increased expression of caspase-1 p20-positive neurons, microglia, and endothelial cells in the hypothalamus, temporal lobe, and parietal lobe at 72 h and 7 d after SAH. The caspase-1 p20-positive astrocytes were limited in the glia limitans on the brain surface near the puncture site at 24 h after SAH, and expression was increased in brain parenchyma in the hypothalamus, temporal lobe, and parietal lobe at 72 h and 7d after SAH. In comparison with Sham group,

quantification analysis (Figure 2e) showed that caspase-1 p20-positive neurons and astrocytes were significantly increased 24 h to 7 d after SAH ($P<0.001$, one-way ANOVA, Tukey's post hoc test); caspase-1 p20-positive microglia were significantly increased 72 h and 7 d after SAH ($P < 0.011$, one-way ANOVA, Tukey's post hoc test). The caspase-1 p20-positive endothelial cells peaked at 24 h and 72 h after SAH ($P<0.006$, one-way ANOVA, Tukey's post hoc test).

The TF-positive cells were primarily observed in glia limitans in the Sham group. The TF expression was further increased in the brain parenchyma at 24 h and 7 d, and peaked at 72 h after SAH when compared to Sham group ($P<0.001$, one-way ANOVA, Tukey's post hoc test) (Figure 2d, e).

Inhibition of caspase-1 accelerated CSF circulation and blood clearance after SAH in rats
The severe blood coagulation in CSF could block CSF circulation, increase brain water content and ICP, as well as deteriorate neurobehavioural function after
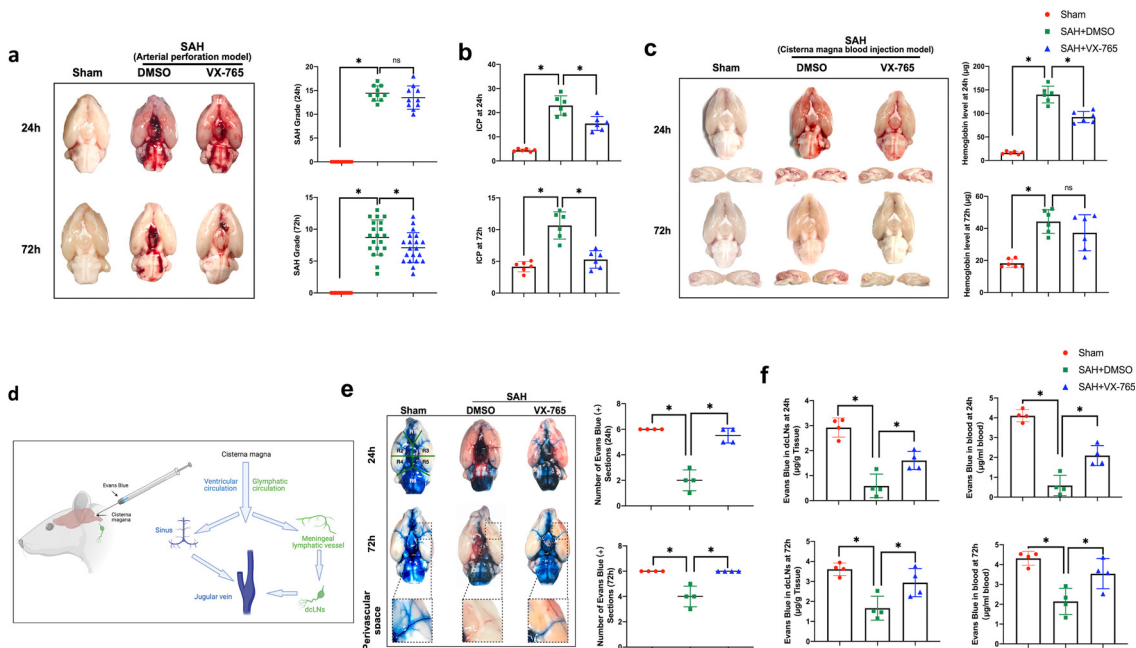
Figure 3. Inhibition of caspase-1 by VX-765 facilitated CSF circulation, accelerated blood clearance, and improved neurological function after SAH in rats. a. Representative image of blood distribution on ventral surface of brain, and SAH grade at 24 h and 72 h after SAH. $n = 10-20$ per group **b.** ICP level at 24 h and 72 h after SAH. $n = 6$ per group **c.** Representative image of blood distribution on ventral surface and ventricle, and cerebral haemoglobin level at 24 h and 72 h after SAH induced by cisterna magna autologous blood injection. $n = 6$ per group **d.** Diagram of EB (2%) cisterna magna injection and subsequent drainage pathways along CSF. **e.** Representative image and quantification of EB distribution in ventral subarachnoid space and perivascular space at 1 h after cisterna magna injection. **f.** Concentration of EB in dcLNs (μg/g tissue) and blood (μg/ml blood) at 1 h after its cisterna magna injection. $n = 4$ per group. All data are presented as mean $\pm$ SD. $* P < 0.05$, ns=no significance. One-way ANOVA, Tukey's post hoc test.

SAH.[17,18] We used neurobehavioural tests and brain water content measurements to determine the best dosage of caspase-1 inhibitor, VX-765 (Figure S2). Compared to the SAH+DMSO group, the VX-765 treatment, at a dosage of 0.6 mg/kg, significantly increased the modified Garcia scores at 24 h after SAH ($P = 0.037$, one-way ANOVA, Tukey's post hoc test). However, VX-765 at neither dosage benefited Beam Balance performance at 24 h after SAH ($P > 0.255$, one-way ANOVA, Tukey's post hoc test). Meanwhile, VX-765, at a dosage of 0.6 mg/kg, significantly decreased brain water content in bilateral hemispheres at 24 h after SAH ($P < 0.033$, two-way ANOVA, Tukey's post hoc test). VX-765 treatment at dosages of 0.6 mg/kg and 1.8 mg/kg markedly increased the modified Garcia scores and Beam Balance scores at 72 h after SAH ($P < 0.029$, one-way ANOVA, Tukey's post hoc test). Similarly, VX-765, at dosages of 0.6 mg/kg and 1.8 mg/kg, markedly decreased brain water content in bilateral hemispheres at 72 h after SAH ($P < 0.021$, two-way ANOVA, Tukey's post hoc test). Therefore, VX-765 treatment, at a dosage 0.6 mg/kg, was used as the best dose for the following experiments.

Visible blood clots were observed depositing on the ventral surface of the brain in DMSO-treated SAH rats, but the clot appeared to resolve in VX-765-treated SAH rats, both at 24 h and 72 h after SAH (Figure 3a). While SAH grades were not statistically significant between SAH + DMSO and SAH + VX-765 at 24 h after SAH ($P = 0.468$, one-way ANOVA, Tukey's post hoc test), the SAH grade at 72 h after SAH was markedly decreased in VX-765-treated SAH rats ($P = 0.049$, one-way ANOVA, Tukey's post hoc test). Of note, the VX-765 treatment decreased the SAH-induced intracranial hypertension at both 24 h and 72 h after SAH ($P < 0.001$, one-way ANOVA, Tukey's post hoc test) (Figure 3b). Considering the relatively inconsistent amount of bleeding in the artery perforation model, the SAH model of cisterna magna autologous blood injection was further used for examining the effect of VX-765 on blood clearance. As the results showed in Figure 3c, in the absence of visible blood clots on the ventral surface (subarachnoid space) or lateral ventricles at 24 h and 72 h after SAH, the brain haemoglobin levels were significantly decreased in VX-765-treated SAH rats at 24 h after SAH ($P < 0.001$, one-way ANOVA, Tukey's post hoc test), and demonstrated a downward trend at 72 h after SAH ($P = 0.300$, one-way ANOVA, Tukey's post hoc test).

EB dye was injected via cisterna magna into the subarachnoid space to trace the CSF circulation. At 1 h after injection, the EB dye was grossly visible on the ventral

surface (subarachnoid space), the perivascular space near the Willis cycle, and its belonging arteries in the Sham group. The spread of EB was quantified according to our previous study.[27] Compared to Sham, the EB-positive section was significantly decreased at 24 h and 72 h after SAH ($P<0.001$, one-way ANOVA, Tukey's post hoc test) (Figure 3e). The VX-765 treatment markedly improved the EB movement and the EB-positive sections at 24 h and 72 h after SAH ($P<0.001$, one-way ANOVA, Tukey's post hoc test) (Figure 3e).

According to the current understanding of the CSF circulation pathway, CSF moves through not only the ventricular system, but also the glymphatic system, which drains into the sinus to enter jugular veins or meningeal lymphatic vessels to end up in dcLNs, respectively.[41] As shown in Figure 3f, the concentration of EB was markedly decreased in the dcLNs and blood at both 24 h and 72 h after SAH when compared to Sham ($P<0.002$, one-way ANOVA, Tukey's post hoc test), suggesting the impaired CSF EB clearance. However, the VX-765 treatment significantly reversed the SAH-induced CSF EB clearance impairment in SAH rats with greater the EB concentration in the dcLNs and blood at both 24 h and 72 h after SAH ($P<0.003$, one-way ANOVA, Tukey's post hoc test).

Inhibition of caspase-1 alleviated inflammasome activation and fibrin deposition after SAH in rats

To investigate the possible mechanism of caspase-1 inhibition-induced improvement of CSF flow after SAH, we explored the role of caspase-1 inhibition in fibrin deposition at 72 h after SAH. The whole brain immunofluorescence of fibrin showed very light fibrin-associated fluorescence on both the ventral and dorsal brain surfaces in the SAH+DMSO group in contrast to shams and VX-765-treated SAH rats (Figure 4a). Additionally, fibrin deposition was further observed on the subarachnoid space near the temporal cortex, MCA, choroid plexus, and the perivascular space after SAH by immunochemistry staining when compared to Sham ($P<0.004$, one-way ANOVA, Tukey's post hoc test). Similarly, VX-765 treatment reduced fibrin deposition after SAH ($P<0.010$, one-way ANOVA, Tukey's post hoc test) (Figure 4b).

Meanwhile, the immunofluorescence staining of caspase-1 p20 and TUNEL showed that VX-765 treatment significantly reduced the SAH-induced increase of caspase-1 p20-positive cells and caspase-1 p20-/TUNEL-positive pyroptotic cells at 72 h after SAH ($P<0.001$, one-way ANOVA, Tukey's post hoc test) (Figure 4c). Western blots were further conducted to measure the protein levels of inflammasomes and activation of the extrinsic coagulation in the ipsilateral hemisphere (Figure 4d). The protein levels of inflammasome activation markers, including caspase-1 p20, GSDMD-C, IL-1β, and IL-18, were found to be significantly increased at 72 h after SAH compared to Sham ($P<0.010$, one-way ANOVA, Tukey's post hoc test), but decreased after VX-765 treatment ($P<0.048$, one-way ANOVA, Tukey's post hoc test). Accompanied with caspase-1 activation, the protein levels of extrinsic coagulation factors, namely TF and fibrin, were increased at 72 h after SAH compared to Sham ($P<0.001$, one-way ANOVA, Tukey's post hoc test), and were reduced following VX-765 treatment ($P<0.004$, one-way ANOVA, Tukey's post hoc test). Consistently, the SAH-induced TF release in CSF was reduced after VX-765 treatment, as detected by the ELISA ($P<0.001$, one-way ANOVA, Tukey's post hoc test) (Figure 4e).

Cleaved GSDMD is the key protein for pore formation and intracellular component release in pyroptosis.[25] To further verify that the post-SAH coagulation is promoted by caspase-1 inflammasome activation and pyroptosis, we used GSDMD-KO CRISPR to knockout the expression of GSDMD prior to SAH induction. As shown in Figure 4f, GSDMD-KO CRISPR had no effects on brain protein levels of GSDMD-C, IL-1β, IL-18, TF, and fibrin in the Sham group when compared to Sham + control CRISPR ($P>0.187$, one-way ANOVA, Tukey's post hoc test). However, the protein levels of GSDMD and GSDMD-C in SAH + GSDMD-KO CRISPR were significantly lower than SAH + control CRISPR ($P<0.001$, one-way ANOVA, Tukey's post hoc test). The protein levels of IL-1β, IL-18, TF, and fibrin were also reduced after GSDMD-KO CRISPR pretreatment in rats with SAH +control CRISPR ($P<0.048$, one-way ANOVA, Tukey's post hoc test). ELISA assay consistently demonstrated that SAH-induced TF release in CSF was reduced by GSDMD-KO CRISPR when compared to SAH+control CRISPR ($P < 0.001$, one-way ANOVA, Tukey's post hoc test) (Figure 4g). In addition, the SAH grades were decreased (Figure 4h), and the neurobehaviour scores were improved (Figure S3) in SAH + GSDMD KO. CRISPR group when compared SAH+control CRISPR ($P<0.031$, one-way ANOVA, Tukey's post hoc test).

Inhibition of caspase-1 improved long-term outcome after SAH in rats

We further evaluated the effects of caspase-1 inhibition on long-term outcomes after SAH. First, the VX-765 treatment markedly improved 28-day survival rate after SAH ($P<0.001$, Log-rank (Mantel-Cox) test) (**Figure S4**). Next, we found that VX-765 attenuated the neurobehavioural deficits. SAH significantly impaired the rotarod test performance at both 5 and 10 RPM acceleration velocity at 1, 2, and 3 weeks after injury when compared to the Sham ($P<0.001$, two-way ANOVA, Tukey's post hoc test) (Figure 5a). VX-765 treatment markedly increased the falling latency of both acceleration velocities at the first 2 weeks ($P<0.045$, two-way ANOVA, Tukey's post hoc test) (Figure 5a) and increased that of the 5 RPM acceleration velocity at the third week when
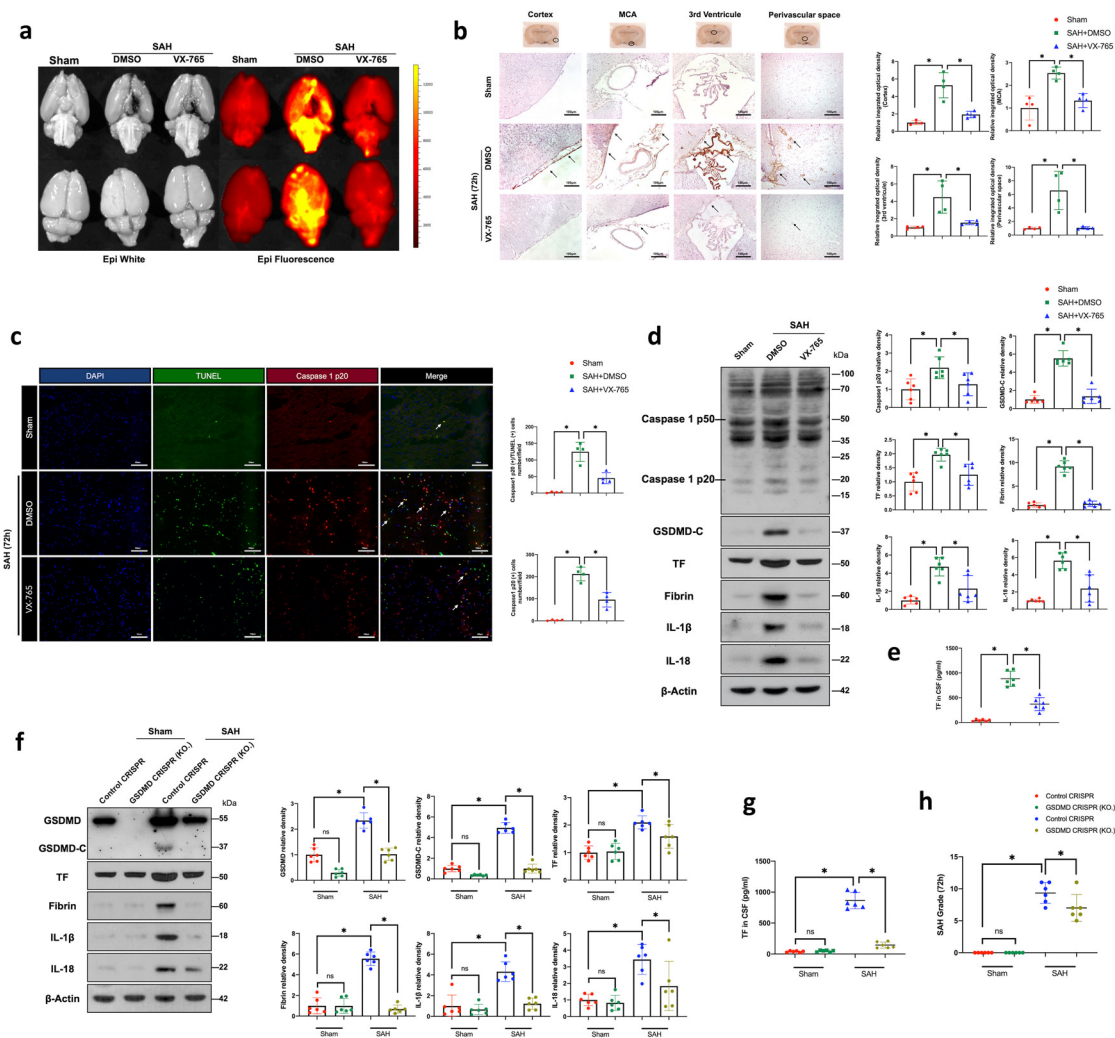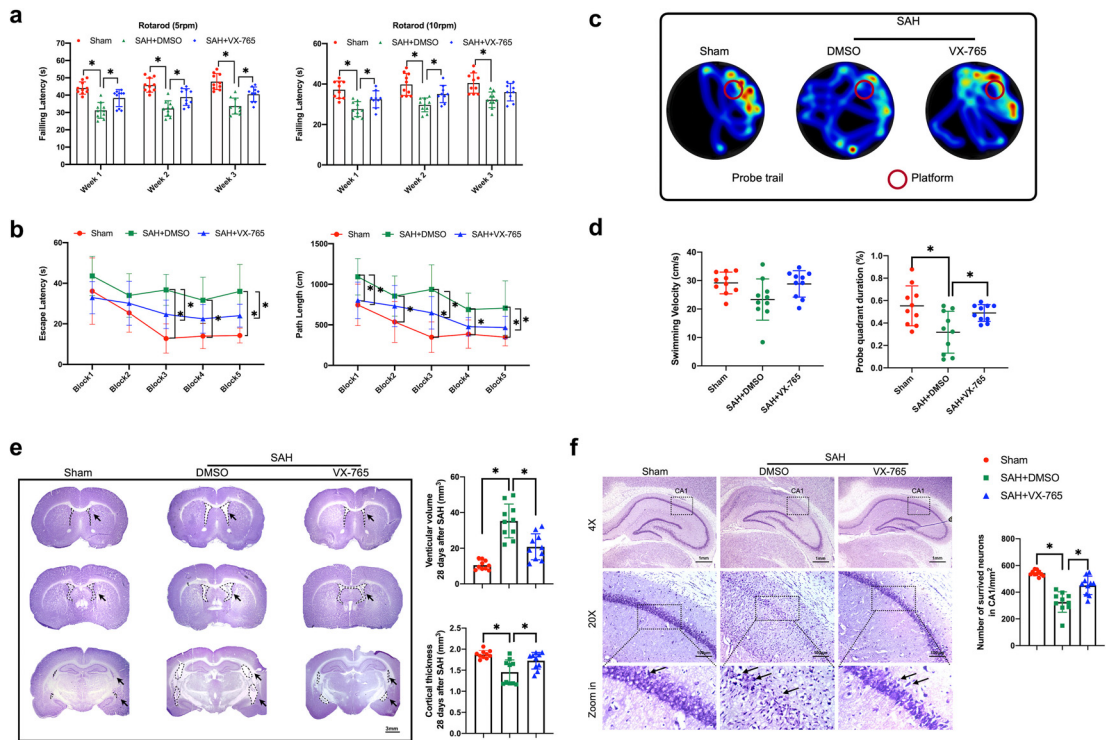
Figure 4. Inhibition of caspase-1 by VX-765 alleviated pyroptotic inflammasome activation and fibrin deposition at 3d after SAH in rats. a. Representative immunofluorescence image of whole brain fibrin. **b.** Representative image and quantification of immunochemistry staining of fibrin near basal cortex, middle cerebral artery (MCA), choroid plexus, and perivascular space after SAH. Positive area was analysed and averaged in three randomised areas for imaging. Scale bar=100 μm. **c.** Representative microphotographs and quantification of co-immunofluorescence staining of caspase-1 p20 (red) with TUNEL (green). Scale bar=100 μm. **d.** Representative western blot bands and densitometric quantification of caspase-1, GSDMD-C, TF, Fibrin, IL-1β, and IL-18 in the ipsilateral hemisphere of Sham, SAH+PBS, and SAH+VX-765. **e.** TF level in CSF after VX-765 treatment, measured by ELISA. **f.** Representative western blot bands and densitometric quantification of GSDMD, GSDMD-C, TF, Fibrin, IL-1β, and IL-18 in the ipsilateral hemisphere of Sham+control CRISPR, Sham+GSDMD CRISPR (KO.), SAH+control CRISPR, and SAH+GSDMD CRISPR (KO.). $n = 6$ per group. **g.** TF level in CSF after GSDMD CRISPR (KO.) administration, measured by ELISA. **h.** SAH grade after GSDMD CRISPR (KO.) administration. The relative level of each protein was normalised to β-actin from the same sample for western blot. $n = 4$ per group for b-c, $n = 6$ per group for d-h. All data are presented as mean $\pm$ SD. *P < 0.05. One-way ANOVA, Tukey's post hoc test.

compared to the SAH+PBS ($P = 0.003$, two-way ANOVA, Tukey's post hoc test) (Figure 5a).

In the Morris water maze test conducted at 4 weeks after injury (Figure 5b), SAH markedly impaired the spatial memory and learning ability with a longer escape latency from days 25 to 27 after SAH ($P<0.001$, two-way ANOVA, Tukey's post hoc test) and swimming distance from days 23 to 27 after SAH to the platform when compared to Sham ($P<0.008$, two-way ANOVA,

Tukey's post hoc test). Compared with rats in SAH +PBS, VX-765 treatment significantly shortened escape latency on days 25 and 27 after SAH ($P < 0.034$, two-way ANOVA, Tukey's post hoc test), with reduced swimming distance on days 23, 25, and 27 after SAH ($P<0.045$, two-way ANOVA, Tukey's post hoc test). In the probe trials, the PBS-treated SAH rats remained in the probe quadrant for a shorter duration than Sham ($P = 0.006$, one-way ANOVA, Tukey's post hoc test)

Figure 5. Inhibition of caspase-1 by VX-765 improved long-term outcomes including neurobehaviour, hydrocephalus, and hippocampal neuronal loss after SAH in rats. **a.** Rotarod test (5RPM and 10 RPM) on the first, second, and third week after SAH. **b.** Escape latency and swimming distance of Morris water maze test on days 23 to 27 after SAH. **c.** Representative thermal imaging of the probe trial. **d.** Quantification of probe quadrant duration and swimming velocities. **e.** Representative images of coronary section at different levels, and quantification of ventricular volume (mm³) and cortical thickness (mm) in different groups Scale bar=3 mm (1.25X). **f.** Representative images and neuronal quantifications of Nissl staining in hippocampal CA1 region. The surviving neurons were counted and averaged in three randomised areas chosen in the ipsilateral cortex for imaging (at 20X magnification). Scale bar=1 mm (4X), 200 μm (20X). $n = 10$/group *$P<0.05$. One-way ANOVA, Tukey's post hoc test for D-f, i-j. Two-way ANOVA, Tukey's post hoc test for a-b.

(Figure 5c, d). VX-765 treatment significantly increased the quadrant duration of SAH rats compared to SAH + PBS ($P = 0.049$, one-way ANOVA, Tukey's post hoc test) (Figure 5c, d). There was no statistical significance in the swimming speed amongst groups in the probe trials ($P>0.060$, one-way ANOVA, Tukey's post hoc test) (Figure 5d).

Inhibition of caspase-1 prevented hydrocephalus and hippocampus neuron loss at 28 d after SAH in rats

Nissl staining was conducted at 28 d after SAH to analyse the morphology of bilateral ventricles and hippocampal neuronal loss. As shown in Figure 5e, SAH significantly induced bilateral ventricular enlargement and reduced cortex thickness when compared to Sham ($P<0.001$, one-way ANOVA, Tukey's post hoc test). VX-765 treatment markedly attenuated SAH-induced ventricular enlargement and cortex attenuation in SAH rats compared to SAH+DMSO ($P<0.004$, one-way ANOVA, Tukey's post hoc test). In the ipsilateral hippocampus

(Figure 5f), SAH significantly reduced the number of neurons in the CA1 area when compared to Sham ($P<0.001$, one-way ANOVA, Tukey's post hoc test). Consistently, VX-765 treatment attenuated SAH-induced neuronal loss in CA1 area when compared to SAH+DMSO ($P<0.001$, one-way ANOVA, Tukey's post hoc test).

Inhibition of caspase-1 reduced haemoglobin-induced astrocyte pyroptosis and TF release in vitro

Using the primary astrocyte culture, the objective of this experiment was to validate that the caspase-1-dependant inflammasome activation enhanced the coagulation response through the astrocytic pyroptosis. Because pyroptotic cells releases intracellular LDH,[38] we used CCK-8 assay and LDH release assay to determine the best dosage of VX-765 against astrocyte pyroptosis in primary astrocyte cultures after haemoglobin exposure. As shown in Figure 6a, while haemoglobin exposure increased astrocyte cell viability ($P<0.001$, one-way
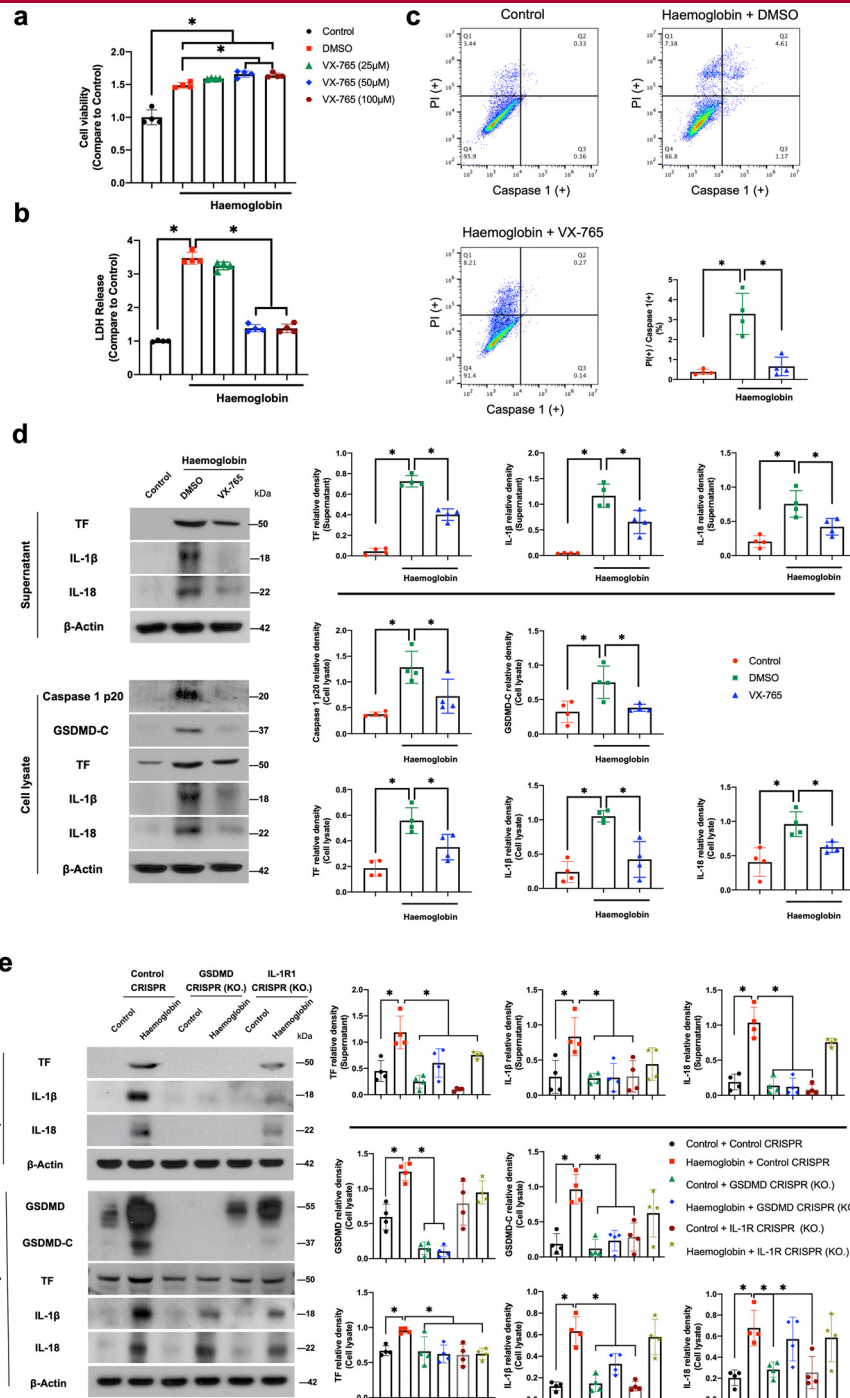
Figure 6. Inhibition of caspase-1 by VX-765 reduced haemoglobin-induced pyroptosis and TF production/release in primary astrocyte culture. a-b. Relative cell viability and LDH level of Control, Haemoglobin+DMSO and Haemoglobin+VX-765 (25 μM, 50 μM and 100 μM). **c.** Representative dots plot and quantification of flow cytometry. Caspase-1(+)/PI(+) represents cells with pyroptosis. **d.** Representative western blot bands and densitometric quantification of caspase-1 p20, GSDMD-C, TF, IL-1β, and IL-18 in supernatant and cell lysate of Control, Haemoglobin+DMSO, and Haemoglobin+VX-765. **e.** Representative western blot bands and densitometric quantification of GSDMD, GSDMD-C, TF, IL-1β, and IL-18 in supernatant and cell lysate of cells of treated with haemoglobin, Control CRISPR, GSDMD CRISPR (KO.), and IL-1R1 CRISPR (KO.). The relative level of each protein was normalised to β-actin from the same sample for western blot. Each experiment was repeated 3 times. All data are presented as mean $\pm$ SD. *$P < 0.05$. One-way ANOVA, Tukey's post hoc test.

ANOVA, Tukey's post hoc test), VX-765, at dosages of 50 μM and 100 μM, further increased the cell viability 24 h after haemoglobin exposure ($P<0.021$, one-way ANOVA, Tukey's post hoc test). In contrast, haemoglobin significantly induced intracellular LDH release when compared with the control group (<0.001, one-way ANOVA, Tukey's post hoc test) (Figure 6b). However, VX-765 treatment, at dosages of 50 μM and 100 μM, attenuated haemoglobin-induced LDH release ($P<0.001$, one-way ANOVA, Tukey's post hoc test). Therefore, the dosage of 50 μM was used for the following study. To further confirm VX-765 attenuated cell pyroptosis, activated caspase-1 and PI were assessed using flow cytometry. The proportion of pyroptotic cells with activated caspase-1 (+)/PI (+) was significantly increased after haemoglobin induction ($P<0.001$, one-way ANOVA, Tukey's post hoc test), but was reduced by VX-765 treatment ($P<0.001$, one-way ANOVA, Tukey's post hoc test) (Figure 6c).

Furthermore, western blot analysis (Figure 6d) of inflammatory cytokines and TF in cell culture supernatant revealed that haemoglobin significantly increased the cell release of IL-1β, IL-18, and TF, when compared to Control ($P<0.05$, one-way ANOVA, Tukey's post hoc test). VX-765 treatment significantly reduced haemoglobin-induced inflammatory cytokines and TF release ($P<0.021$, one-way ANOVA, Tukey's post hoc test). In cell lysates, the protein levels of caspase-1 p20, cleaved GSDMD, inflammatory cytokines, and TF were also significantly increased by haemoglobin ($P<0.003$, one-way ANOVA, Tukey's post hoc test) which were reduced by VX-765 treatment ($P<0.043$, one-way ANOVA, Tukey's post hoc test).

### GSDMD facilitated TF release and IL-1R1 promoted TF upregulation in astrocytes in vitro

We used GSDMD-KO CRISPR to explore the role of GSDMD and inflammatory cytokines in TF production and release after haemoglobin exposure in primary astrocyte culture. Western blots (Figure 6e) revealed that GSDMD-KO CRISPR had no effect on control group when compared to Control+control CRISPR in expression levels of cytokines and TF ($P>0.999$, one-way ANOVA, Tukey's post hoc test). In contrast, the GSDMD-KO CRISPR significantly reduced GSDMD and GSDMD-C in cell lysates of Haemoglobin +GSDMD-KO CRISPR, when compared to Haemoglobin+control CRISPR ($P<0.001$, one-way ANOVA, Tukey's post hoc test). In addition, when compared to Haemoglobin+control CRISPR, GSDMD-KO CRISPR not only significantly abolished haemoglobin-induced IL-1β, IL-18, and TF release to supernatant of cell culture ($P<0.013$, one-way ANOVA, Tukey's post hoc test), but also the haemoglobin-induced IL-1β and TF production in cell lysate ($P<0.165$, one-way ANOVA, Tukey's post hoc test).

IL-1β is proposed as a potent transcription promoter of TF.[24] Given the significant high IL-1β in supernatant after astrocytes exposure to haemoglobin, we used IL-1R1-KO CRISPR to further explore the mechanism of IL-1β/IL-1R1 signalling, which in turn promoted TF production in cell lysate after haemoglobin exposure. As shown in Figure 6e, IL-1R1-KO CRISPR had no effect on control group when compared to control+control CRISPR in expression levels of cytokines and TF ($P>0.999$, one-way ANOVA, Tukey's post hoc test). The haemoglobin-induced overproduction of TF in cell lysate was abolished by the IL-1R1-KO CRISPR when compared to Haemoglobin+control CRISPR ($P<0.017$, one-way ANOVA, Tukey's post hoc test).

Discussion

This study revealed caspase-1 as a link between pyroptosis-related neuroinflammation and the blood coagulation response in the brain after SAH. Pharmacological inhibition of caspase-1 by VX-765 could alleviate the release of neuroinflammatory cytokines and extrinsic coagulation factor TF from pyroptosis after SAH. Specifically, the main findings are listed as follows: 1) Inflammatory and coagulation responses are activated in human CSF after SAH. The caspase-1 levels significantly correlated with the levels of extrinsic coagulation factors and pyroptosis-related cytokines, as well as with clinical severity and outcome at discharge; 2) The expression of caspase-1 with its cleaved form were markedly increased on neurons, microglia, astrocytes, and endothelial cells after SAH in rats. Meanwhile, the expression of coagulation-related TF was primarily increased on astrocytes after SAH in rats; 3) Intranasal administration of caspase-1 inhibitor, VX-765, significantly attenuated neurological deficits and brain oedema at 24 h and 72 h after SAH. Such benefits were accompanied by accelerated CSF circulation, quicker blood clearance, less pyroptotic neuroinflammation, and reduced TF-induced fibrin deposition in SAH rats; 4) Administration of VX-765 improved long-term outcomes, including survival rate, motor coordination, spatial learning and memory with less hippocampal neuronal loss and hydrocephalus in SAH rats; 5) Administration of VX-765 reduced haemoglobin-induced pyroptosis, as well as TF production/release in primary astrocyte cultures. The detailed schematic of the proposed mechanisms is shown as Figure 7.

Accumulating clinical and preclinical research has focused on anti-neuroinflammation and anti-blood coagulation in CSF after SAH in past decades, which highlights the important roles of neuroinflammation and blood clot deposition in the post-SAH pathological process.[8,9,11,17,42] The benefit of either intraventricular fibrinolysis or inflammatory cytokine antagonist administration in SAH patients has been demonstrated in several clinical trials.[17,42] Consistently, we detected the
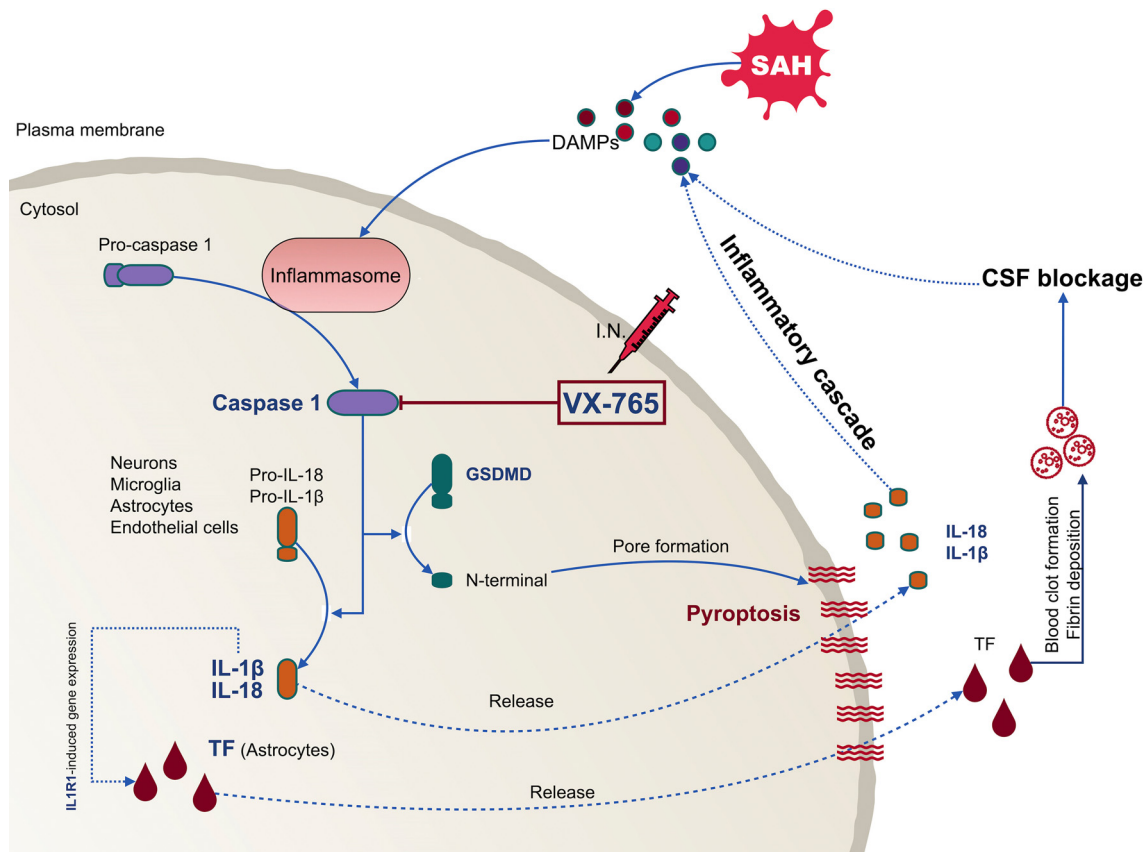
Figure 7. Schematic of Proposed Mechanisms.

activated inflammatory and coagulation responses in the CSF samples of SAH patients by proteomic analysis. amongst all, fibrinogen alpha chain, fibrinogen beta chain, fibrinogen gamma chain, and IL-1R1 were the top upregulated proteins in CSF after SAH. Fibrinogen chains are the critical markers for fibrin clot formation triggered by the coagulation pathway. The coagulation could be initiated by the exposed collagen in the coagulation factor XII-dependant intrinsic pathway or by tissue injury in TF-depended extrinsic pathway.[43] IL-1R1 is the surface membrane receptor for IL-1β and IL-1α of neural cells, which may travel into the CSF upon cell degradation after programmed cell death, such as pyroptosis.[44] Our findings reaffirmed the critical roles of fibrin and IL-1β in the pathological process after SAH.

Caspase-1-dependant inflammasome activation contributes to the neuroinflammatory response after SAH, which aggravates maturation and release of pro-inflammatory cytokines, IL-1β and IL-18, as well as host cell death.[20] Of interest, caspase-1-dependant inflammasome activation in macrophages has been shown to cause intravascular TF release and trigger fibrin clotting.[25] Recent clinical studies also revealed a correlation between the levels of caspase-1 and TF in CSF with the

clinical outcome of SAH patients. The higher caspase-1 levels in the CSF of SAH patients correlated with worse functional outcome.[45] The elevation of CSF TF was predictive of cerebral vasospasm and poor outcomes in SAH patients.[46] In our study, the sensitive ELISA approach demonstrated that the higher caspase-1 levels corresponded to the higher levels of TF, TAT, fibrin, and IL-1β in CSF of SAH patients. Meanwhile, the brain protein levels of caspase-1-dependant inflammasomes and extrinsic coagulation cascade increased from 24 h to 7 d after SAH in rats. Caspase-1, therefore, appears to be an ideal therapeutic target to alleviate both neuroinflammation- and TF-mediated blood clot deposition after SAH.

Caspase-1 is widely activated in neurons, astrocytes, endothelial cells, and microglia after acute brain injury.[47] Our results consistently demonstrated that the upregulated caspase-1 p20 was primarily expressed in neurons and astrocytes at 3 d after SAH in rats. VX-765 is a potent selective caspase-1 inhibitor that acts via covalent modification of the catalytic cysteine residue in the active site of caspase-1. It was well-tolerated in a phase II trial as a potential treatment for epilepsy (NCT01501383).[48] Previous studies have demonstrated that the caspase-1 inhibition by VX-765 significantly

improved neurological outcome via attenuating neuro-inflammation and neuronal pyroptosis in rodent models of traumatic brain injury and cerebral ischaemia.[49,50] Similarly, we also demonstrated that intranasal VX-765 treatment presented potent short- and long-term neuroprotective effects by attenuating neuronal pyroptosis and proinflammatory cytokines after SAH in rats.

Besides, we found that VX-765 treatment also down-regulated the production and release of brain TF to the CSF after SAH. TF release in CSF occurs after brain tissue injury, which initiates the extrinsic coagulation pathway and fibrin clotting. Fibrin deposition in the subarachnoid space, perivascular space, and lateral ventricles directly blockage CSF circulation with fibrin deposition on choroid plexuses causing CSF hypersecretion.[11,15] Therefore, the caspase-1 inhibition by VX-765 treatment decreased fibrin deposition in the CSF circulation pathway, which accelerated CSF movement and blood clearance at 3 d after SAH, as well as prevented hydrocephalus formation at 28 d after SAH in rats. Similarly, the blood clearance rate was also found accelerated by VX-765 treatment in cisterna magna autologous blood injection model at 1 d rather 3 d after SAH, which may be resulted by the less blood and reduced physical brain injury of this model.[31]

Astrocytes, the critical cell type for cerebral wound healing, express high levels of TF in the CNS.[43,51] We observed the co-localisation of TF and activated caspase-1 in astrocytes from 1 d to 3 d after SAH in rats. Inhibition of caspase-1 by VX-765 successfully attenuated TF and inflammatory cytokine release via GSDMD cleavage-mediated membrane pore formation in a haemoglobin-stimulated astrocytic cell line. Given that inflammatory cytokine, IL-1β, was released along cell pyroptosis, it could promote TF transcription in monocytes and endothelial cells through IL-1β/IL-1R1 signalling.[24] Such mechanism of inflammation-regulated TF production likely occurred in astrocytes after SAH as well. Thus, these results suggest that caspase-1 inhibition could be effective in attenuating neuroinflammation and TF-activated blood-coagulation response after SAH.

There are several limitations in our study. First, we could not exclude endothelial cells as another source of TF released into the subarachnoid space. Nevertheless, the major source of TF in CSF appears to be contributed by astrocytes as previously reported.[26] Second, although VX-765 is recommended as a potent selective inhibitor of caspase-1, a transgenic caspase-1 knockout animal model is still needed to further validate our current findings. Third, we did not address the gender difference by using only male rats. Fourth, the limited small sample sizes may introduce some potential bias.

In conclusion, caspase-1 is a key factor responsible for both neuroinflammation and TF-mediated blood coagulation via pyroptosis after SAH. Pharmacological inhibition of caspase-1 by VX-765 alleviated the releases of proinflammatory cytokines from pyroptotic neural cells and extrinsic coagulation initiator TF from pyroptotic astrocytes, which reduced fibrin clotting in CSF and CSF flow blockage leading to better neurological outcomes after experimental SAH. Thus, inhibition of caspase-1 via VX-765 may serve as a potential new treatment for SAH.

Declaration of interests
The authors declare no conflict of interest concerning the materials used in this study or findings specified in this paper.

Contributors
Y.F, J.H.Z, J.Z, J.T, and S.C contributed to the design of study. Y.F, X.W performed the clinical sample collection and statistical analysis. J.L, H.S, and A.S conducted the western blot and statistical analysis. A.Z, Y.L, and R.R carried out the histological staining and statistical analysis. A.Z and Y.L conducted the in vitro experiments. Y.F, L.H, and C.L wrote the manuscript. Y.F, J.L and X.W verified the underlying data. All authors read and approved the final version of the manuscript.

Data sharing statement
The mass spectrometry proteomics data have been deposited to the ProteomeXchange Consortium via the PRIDE partner repository with the dataset identifier PXD030593. The full blots (with labelling) for all blots that appear in the manuscript are in Supplemental Western blots. Readers are welcome to contact the corresponding author for the raw data used in this work.

Supplementary materials
Supplementary material associated with this article can be found in the online version at doi:10.1016/j.ebiom.2022.103843.

References

1 Lawton MT, Vates GE. Subarachnoid hemorrhage. *N Engl J Med*. 2017;377(3):257–266.
2 Jabbarli R, Reinhard M, Niesen WD, et al. Predictors and impact of early cerebral infarction after aneurysmal subarachnoid hemorrhage. *Eur J Neurol*. 2015;22(6):941–947.
3 Aldrich EF, Higashida R, Hmissi A, et al. Thick and diffuse cisternal clot independently predicts vasospasm-related morbidity and poor outcome after aneurysmal subarachnoid hemorrhage. *J Neurosurg*. 2020:1–9.
4 Petridis AK, Kamp MA, Cornelius JF, et al. Aneurysmal Subarachnoid Hemorrhage. *Dtsch Arztebl Int*. 2017;114(13):226–236.
5 Fang Y, Shao Y, Lu J, et al. The effectiveness of lumbar cerebrospinal fluid drainage in aneurysmal subarachnoid hemorrhage with different bleeding amounts. *Neurosurg Rev*. 2020;43(2):739–747.
6 Gigante P, Hwang BY, Appelboom G, et al. External ventricular drainage following aneurysmal subarachnoid haemorrhage. *Br J Neurosurg*. 2010;24(6):625–632.
7 Doczi T, Nemessanyi Z, Szegvary Z, Huszka E. Disturbances of cerebrospinal fluid circulation during the acute stage of subarachnoid hemorrhage. *Neurosurgery*. 1983;12(4):435–438.
8 Gaberel T, Gakuba C, Goulay R, et al. Impaired glymphatic perfusion after strokes revealed by contrast-enhanced MRI: a new target for fibrinolysis? *Stroke*. 2014;45(10):3092–3096.
9 Siler DA, Gonzalez JA, Wang RK, Cetas JS, Alkayed NJ. Intracisternal administration of tissue plasminogen activator improves cerebrospinal fluid flow and cortical perfusion after subarachnoid hemorrhage in mice. *Transl Stroke Res*. 2014;5(2):227–237.
10 Milhorat TH. Acute hydrocephalus after aneurysmal subarachnoid hemorrhage. *Neurosurgery*. 1987;20(1):15–20.
11 Golanov EV, Bovshik EI, Wong KK, et al. Subarachnoid hemorrhage - Induced block of cerebrospinal fluid flow: role of brain coagulation factor III (tissue factor). *J Cereb Blood Flow Metab*. 2018;38(5):793–808.
12 Hinson HE, Hanley DF, Ziai WC. Management of intraventricular hemorrhage. *Curr Neurol Neurosci Rep*. 2010;10(2):73–82.
13 Chopard RP, Brancalhao RC, Miranda-Neto MH, Biazotto W. Arachnoid granulation affected by subarachnoid hemorrhage. *Arq Neuropsiquiatr*. 1993;51(4):452–456.
14 Luo C, Yao X, Li J, et al. Paravascular pathways contribute to vasculitis and neuroinflammation after subarachnoid hemorrhage independently of glymphatic control. *Cell Death Dis*. 2016;7:e2160.
15 Mayfrank L, Kim Y, Kissler J, et al. Morphological changes following experimental intraventricular haemorrhage and intraventricular fibrinolytic treatment with recombinant tissue plasminogen activator. *Acta Neuropathol*. 2000;100(5):561–567.
16 Pu T, Zou W, Feng W, et al. Persistent malfunction of glymphatic and meningeal lymphatic drainage in a mouse model of subarachnoid hemorrhage. *Exp Neurobiol*. 2019;28(1):104–118.
17 Sasaki T, Kodama N, Kawakami M, et al. Urokinase cisternal irrigation therapy for prevention of symptomatic vasospasm after aneurysmal subarachnoid hemorrhage: a study of urokinase concentration and the fibrinolytic system. *Stroke*. 2000;31(6):1256–1262.
18 Ramakrishna R, Sekhar LN, Ramanathan D, et al. Intraventricular tissue plasminogen activator for the prevention of vasospasm and hydrocephalus after aneurysmal subarachnoid hemorrhage. *Neurosurgery*. 2010;67(1):110–117. discussion 7.
19 Coulibaly AP, Provencio JJ. Aneurysmal subarachnoid hemorrhage: an overview of inflammation-induced cellular changes. *Neurotherapeutics*. 2020;17(2):436–445.
20 Yuan B, Zhou XM, You ZQ, et al. Inhibition of AIM2 inflammasome activation alleviates GSDMD-induced pyroptosis in early brain injury after subarachnoid haemorrhage. *Cell Death Dis*. 2020;11(1):76.
21 Walsh JG, Muruve DA, Power C. Inflammasomes in the CNS. *Nat Rev Neurosci*. 2014;15(2):84–97.
22 Levi M, van der Poll T. Inflammation and coagulation. *Crit Care Med*. 2010;38(2 Suppl):S26–S34.
23 Chanchal S, Mishra A, Singh MK, Ashraf MZ. Understanding inflammatory responses in the manifestation of prothrombotic phenotypes. *Front Cell Dev Biol*. 2020;8:73.
24 Bode M, Mackman N. Regulation of tissue factor gene expression in monocytes and endothelial cells: thromboxane A2 as a new player. *Vascul Pharmacol*. 2014;62(2):57–62.

25 Wu C, Lu W, Zhang Y, et al. Inflammasome activation triggers blood clotting and host death through pyroptosis. *Immunity*. 2019;50(6). 1401–11 e4.
26 Wang S, Reeves B, Pawlinski R. Astrocyte tissue factor controls CNS hemostasis and autoimmune inflammation. *Thromb Res*. 2016;141(Suppl 2):S65–S67.
27 Fang Y, Shi H, Ren R, et al. Pituitary adenylate cyclase-activating polypeptide attenuates brain edema by protecting blood-brain barrier and glymphatic system after subarachnoid hemorrhage in rats. *Neurotherapeutics*. 2020;17(4):1954–1972.
28 Fang Y, Shao A, Wang X, et al. Deep venous drainage variant rate and degree may be higher in patients with perimesencephalic than in non-perimesencephalic angiogram-negative subarachnoid hemorrhage. *Eur Radiol*. 2021;31(3):1290–1299.
29 Niknejad SIaMT. Sentinel clot sign; 2021. [Available from: https://radiopaedia.org/articles/sentinel-clot-sign?lang=us.
30 Yang Y, Ren J, Sun Y, et al. A connexin43/YAP axis regulates astroglial-mesenchymal transition in hemoglobin induced astrocyte activation. *Cell Death Differ*. 2018;25(10):1870–1884.
31 Prunell GF, Mathiesen T, Diemer NH, Svendgaard NA. Experimental subarachnoid hemorrhage: subarachnoid blood volume, mortality rate, neuronal death, cerebral blood flow, and perfusion pressure in three different rat models. *Neurosurgery*. 2003;52(1):165–175. discussion 75-6.
32 Sugawara T, Ayer R, Jadhav V, Zhang JH. A new grading system evaluating bleeding scale in filament perforation subarachnoid hemorrhage rat model. *J Neurosci Methods*. 2008;167(2):327–334.
33 Tang XN, Berman AE, Swanson RA, Yenari MA. Digitally quantifying cerebral hemorrhage using Photoshop and Image J. *J Neurosci Methods*. 2010;190(2):240–243.
34 Erdo F, Bors LA, Farkas D, Bajza A, Gizurarson S. Evaluation of intranasal delivery route of drug administration for brain targeting. *Brain Res Bull*. 2018;143:155–170.
35 PubChem Compound Summary for CID 11398092. *Belnacasan. Nat Center Biotechnol Inf*. 2021. [Available from: https://pubchem.ncbi.nlm.nih.gov/compound/Belnacasan.
36 Flores J, Noel A, Foveau B, et al. Caspase-1 inhibition alleviates cognitive impairment and neuropathology in an Alzheimer's disease mouse model. *Nat Commun*. 2018;9(1):3916.
37 Wolf MS, Chen Y, Simon DW, et al. Quantitative and qualitative assessment of glymphatic flux using Evans blue albumin. *J Neurosci Methods*. 2019;311:436–441.
38 Liu YG, Chen JK, Zhang ZT, et al. NLRP3 inflammasome activation mediates radiation-induced pyroptosis in bone marrow-derived macrophages. *Cell Death Dis*. 2017;8(2):e2579.
39 Investigate the Relationship Between Inflammatory and Coagulation in SAH CSF ClinicalTrials.gov; 2022. [Available from: https://clinicaltrials.gov/ct2/show/NCT04938414.
40 Ahn SH, Savarraj JP, Pervez M, et al. The subarachnoid hemorrhage early brain edema score predicts delayed cerebral ischemia and clinical outcomes. *Neurosurgery*. 2018;83(1):137–145.
41 Bothwell SW, Janigro D, Patabendige A. Cerebrospinal fluid dynamics and intracranial pressure elevation in neurological diseases. *Fluids Barriers CNS*. 2019;16(1):9.
42 Galea J, Ogungbenro K, Hulme S, et al. Reduction of inflammation after administration of interleukin-1 receptor antagonist following aneurysmal subarachnoid hemorrhage: results of the Subcutaneous Interleukin-1Ra in SAH (SCIL-SAH) study. *J Neurosurg*. 2018;128(2):515–523.
43 Golanov EV, Sharpe MA, Regnier-Golanov AS, et al. Fibrinogen chains intrinsic to the brain. *Front Neurosci*. 2019;13:541.
44 Fang Y, Gao S, Wang X, et al. Programmed cell deaths and potential crosstalk with blood−brain barrier dysfunction after hemorrhagic stroke. *Front. Cell Neurosci.*. 2020;14(68).
45 Hirsch Y, Geraghty JR, Katz EA, Testai FD. Inflammasome caspase-1 activity is elevated in cerebrospinal fluid after aneurysmal subarachnoid hemorrhage and predicts functional outcome. *Neurocrit Care*. 2021;34(3):889–898.
46 Hirashima Y, Nakamura S, Suzuki M, et al. Cerebrospinal fluid tissue factor and thrombin-antithrombin III complex as indicators of tissue injury after subarachnoid hemorrhage. *Stroke*. 1997;28(9):1666–1670.
47 Gong Z, Pan J, Shen Q, Li M, Peng Y. Mitochondrial dysfunction induces NLRP3 inflammasome activation during cerebral ischemia/reperfusion injury. *J Neuroinflammation*. 2018;15(1):242.

48 McKenzie BA, Mamik MK, Saito LB, et al. Caspase-1 inhibition prevents glial inflammasome activation and pyroptosis in models of multiple sclerosis. *Proc Natl Acad Sci U S A.* 2018;115(26):E6065–E6E74.

49 Li Q, Dai Z, Cao Y, Wang L. Caspase-1 inhibition mediates neuroprotection in experimental stroke by polarizing M2 microglia/macrophage and suppressing NF-kappaB activation. *Biochem Biophys Res Commun.* 2019;513(2):479–485.

50 Sun Z, Nyanzu M, Yang S, et al. VX765 attenuates pyroptosis and HMGB1/TLR4/NF-kappaB pathways to improve functional outcomes in TBI mice. *Oxid Med Cell Longev.* 2020;2020: 7879629.

51 Eddleston M, de la Torre JC, Oldstone MB, et al. Astrocytes are the primary source of tissue factor in the murine central nervous system. A role for astrocytes in cerebral hemostasis. *J Clin Invest.* 1993;92(1):349–358.